HHS Public Access

Author manuscript

Nat Genet. Author manuscript; available in PMC 2015 February 01.

Published in final edited form as:

Nat Genet. 2014 August ; 46(8): 905–911. doi:10.1038/ng.3031.

The oral-facial-digital syndrome gene *C2CD3* encodes a positive regulator of centriole elongation

Christel Thauvin-Robinet[1,2,17], **Jaclyn S. Lee**[3,17], **Estelle Lopez**[1], **Vicente Herranz-Pérez**[4,5], **Toshinobu Shida**[3], **Brunella Franco**[6,7], **Laurence Jego**[1], **Fan Ye**[3], **Laurent Pasquier**[8], **Philippe Loget**[9], **Nadège Gigot**[1,10], **Bernard Aral**[1,10], **Carla A.M. Lopes**[11], **Judith St-Onge**[1,10], **Ange-Line Bruel**[1], **Julien Thevenon**[1,2], **Susana González-Granero**[4,5], **Caroline Alby**[12,13], **Arnold Munnich**[13,14], **Michel Vekemans**[12,13,14], **Frédéric Huet**[1,2], **Andrew M. Fry**[11], **Sophie Saunier**[13,15], **Jean-Baptiste Rivière**[1,10], **Tania Attié-Bitach**[12,13,14], **Jose Manuel Garcia-Verdugo**[4,5], **Laurence Faivre**[1,2], **André Mégarbané**[16], and **Maxence V. Nachury**[3]

[1]EA GAD, IFR Santé – STIC, Université de Bourgogne, Dijon, France

[2]Centre de Référence Maladies Rares « Anomalies du Développement et Syndromes malformatifs » de l'Est, Centre de Génétique et Pédiatrie 1, Hôpital d'Enfants, CHU Dijon, France

[3]Department of Molecular and Cellular Physiology, Stanford University School of Medicine, Stanford, CA, USA

[4]Laboratorio de Neurobiología Comparada, Instituto Cavanilles, Universitat de València, CIBERNED, Spain

[5]Unidad mixta de Esclerosis múltiple y neurorregeneración, IIS Hospital La Fe-UVEG, Valencia, Spain

[6]Telethon Institute of Genetics and Medicine-TIGEM, Naples Italy

[7]Department of Medical Translational Sciences, Division of Pediatrics, Federico II University of Naples, Italy

[8]Centre de Référence Maladies Rares « Anomalies du Développement et Syndromes malformatifs » de l'Ouest, Unité Fonctionnelle de Génétique Médicale, CHU Rennes, France

[9]Laboratoire d'Anatomie-Pathologie, CHU Rennes, France

Corresponding Authors: Correspondence should be addressed to M.V.N (nachury@stanford.edu) and C.T-R. (christel.thauvin@chu-dijon.fr).

[17]These authors contributed equally to this work

AUTHOR CONTRIBUTIONS

M.V.N. conceived and supervised the functional characterization of C2cd3. C.T-R designed and conducted the gene identification strategy with assistance from T.A.B., B.F., L.F., L.J., E.L., J.B.R., C.A., N.G., B.A. A.M, J.T., J.S. and A–L.B; J.B.R. and S.S. performed mapping analysis, genetic screening and mutation analysis; A.M., B.F., L.P., P.L. and C.T-R. identified and recruited subjects. S.G-G., A.M., F.H. and M.V. gave technical support and conceptual advice. A.M.F and C.A.M.L provided Ofd1 reagents. M.V.N, J.S.L., T.S. designed, executed and analyzed the immunohistochemistry, overexpression and protein interaction assays. F.Y designed and executed the centriole length measurement by light microscopy. V.H.P and J.M.G.V. designed and executed electron microscopy imaging and analysis. C.T-R. and M.V.N. wrote the manuscript. All the authors reviewed the manuscript.

COMPETING FINANCIAL INTERESTS

The authors declare no competing financial interests.

[10]Laboratoire de Génétique moléculaire, Plateau Technique de Biologie, CHU Dijon, France

[11]Department of Biochemistry, University of Leicester, UK

[12]INSERM U781, Institut IMAGINE, Hôpital Necker-Enfants Malades, Paris, France

[13]Paris Descartes - Sorbonne Paris Cité University, Imagine Institute, Paris, France

[14]Département de Génétique, Hôpital Necker-Enfants Malades, AP-HP, Paris, France

[15]INSERM, UMR-S 1163, Laboratory of Inherited Kidney Diseases, Paris, France

[16]Unité de Génétique Médicale, Faculté de Médecine, Université Saint-Joseph, Beirut, Lebanon

Introductory Paragraph

Centrioles are microtubule-based barrel-shaped structures that initiate the assembly of centrosomes and cilia[1,2]. How centriole length is precisely set remains elusive. The microcephaly protein CPAP/MCPH6 promotes procentriole growth[3–5] while the oral-facial-digital syndrome protein OFD1 represses centriole elongation[6,7]. Here, we uncover a novel subtype of OFD with severe microcephaly and cerebral malformations and identify distinct mutations in two families in the evolutionarily conserved C2CD3 gene. Concordant with the clinical overlap, C2cd3 co-localizes with Ofd1 at the distal end of centrioles and C2CD3 physically associates with OFD1. However, in opposition to Ofd1, loss of C2cd3 results in the shortening of centrioles and the loss of sub-distal and distal appendages. Since C2cd3 overexpression triggers centriole hyperelongation and Ofd1 antagonizes this activity, we propose that C2cd3 directly promotes centriole elongation and that Ofd1 acts as a negative regulator of C2cd3. Our results identify centriole length regulation as an emerging pathomechanism in ciliopathies.

Results and Discussion

Oral-facial-digital syndromes (OFD) are ciliopathies characterized by malformations of the face, oral cavity, and digits[8]. A 4-year-old male patient born from consanguineous parents presented with canonical OFD syndrome as well as severe microcephaly, micropenis and severe intellectual disability (Fig. 1a, b and Supplementary Table 1), indicative of an unclassified OFD syndrome. Brain MRI revealed the presence of Molar Tooth Sign (MTS, a cerebellar anomaly characteristic of Joubert syndrome (JBTS) and related disorders[9]), and several other cerebral malformations (Fig. 1c–e and Supplementary Table 1). His younger sister presented with similar anomalies and cardiac malformation, leading to neonatal death. Homozygosity mapping revealed a candidate region of 4 Mb at 11q13.4-q14.1 (Supplementary Fig. 1a), and coupled exome sequencing identified a homozygous nonsense mutation in the C2CD3 gene (NM_015531.4: c.184C>T; p.Arg62* in exon 2), which was confirmed by Sanger sequencing and was found heterozygous in his parents (Supplementary Fig. 1b).

We next screened the coding exons of *C2CD3* for mutations in 34 OFD patients negative for mutations in known OFD-associated genes. We identified a male fetus with compound heterozygous *C2CD3* mutations consisting of one missense variation (NM_015531.4:c.

3085T>G; p.Cys1029Gly) and a substitution in the splice acceptor consensus sequence of exon 22 (NM_015531.4:c.3911-2A>T). Transcript analysis from the affected fetus showed that the c.3911-2A>T substitution causes splicing of the 5'-end of exon 22 to a downstream cryptic splice site, which leads to a four nucleotide frameshift deletion (NM_015531.4:c.3911_3914delCAAG; p.Ala1304Valfs*3) (Supplementary Fig. 1c–e). In close similarity to the index patient, the second patient exhibited severe microcephaly combined with canonical OFD symptoms (Fig. 1f–j and Supplementary Table 1). Both mutations were absent in the Exome Variant Server (see **URLs**), and were predicted to be damaging according to Human Splicing Finder or PolyPhen2 (see **URLs**).

C2CD3 encodes a protein with seven C2 domains that is universally conserved in organisms that assemble centrioles or cilia[10] (Fig. 1k). A *C2cd3* mutant named *Hearty* (*Hty*) was isolated in a screen for Hedgehog signalling in mice and ciliogenesis is severely compromised in *C2cd3*^{Hty} (hypomorph) or *C2cd3*^{Gt} (null) animals[11] (Fig. 1k). In remarkable resemblance to OFD syndromes, *C2cd3*^{Hty} and *C2cd3*^{Gt} mice exhibit embryonic lethality, exencephaly in the midbrain and posterior forebrain with a characteristic tight mesencephalic flexure, a twisted body axis, pericardial edema, rightward turned heart, and severe polydactyly in all four limbs[11,12]. Thus, together with our finding of *C2CD3* mutations in two unrelated OFD patients, these results demonstrate that *C2CD3* mutations cause OFD. Based on the unique features of microcephaly and cerebral malformations of the two OFD patients with C2CD3 mutations reported here, we propose the name *OFD14* for *C2CD3*. Together with mutations in TMEM216 reported in Joubert (JBTS2, MIM608091), Meckel-Gruber syndrome (MKS2, MIM603194), and OFD VI (Ref. 13), mutations in *C5orf42* in Joubert (JBTS17, MIM614615) and OFD VI (Ref. 14,15) and mutations in *TCTN3* identified in OFD IV (OFD4, MIM258860), MKS and JBTS (Ref. 16), our identification of a new OFD subtype with severe cerebral malformations including MTS further reinforces the clinical continuum of the ciliopathy spectrum and the inclusion of OFD in the ciliopathies.

Besides its requirement for cilium assembly[11], the function of C2cd3 remains largely elusive. A first clue was provided by the mass spectrometry-based identification of C2CD3 as a BBSome-interacting protein (Fig. 1k and Supplementary Fig. 2a). The BBSome is a complex of proteins mutated in the ciliopathy Bardet-Bield Syndrome (BBS, MIM209900) present in cilia and cytoplasmic granules named centriolar satellites[17–20]. To localize C2cd3, we stably expressed GFP-C2cd3 at low levels in a stable clone of mouse IMCD3-FlpIn kidney cells. While C2cd3 was never detected inside cilia, we detected a robust co-localization of C2cd3 with the core centriolar satellite component PCM-1 (Supplementary Fig. 2b). However, knockdown of *C2CD3* in RPE1-hTERT cells and *C2cd3* mutations in immortalized mouse embryonic fibroblasts (MEFs) failed to reveal defects in centriolar satellite function (Supplementary Fig. 2c).

Besides its localization to centriolar satellites, we consistently found C2cd3 at two to four bright juxtanuclear foci that did not overlap with PCM-1 (Supplementary Fig. 2b, insets). Co-staining with a monoclonal antibody against glutamylated tubulin (GT335) –a modified tubulin found at centrioles and ciliary axonemes– revealed these PCM-1-negative foci of C2cd3 to be centrioles (Supplementary Fig. 3a). Although centriolar satellites deliver

proteins such as pericentrin to the centrosome[17,21], inhibiting the movement of centriolar satellites using the microtubule poison nocodazole did not affect C2cd3 abundance at centrioles (Supplementary Fig. 3b).

We then mapped the precise location of C2cd3 within centrioles. We frequently observed two juxtaposed dots of C2cd3 associated with a single spot of glutamylated tubulin (Fig. 2a). Since the two juxtaposed foci of C2cd3 were each positive for centrin, which marks the distal lumen of mature and pro- centrioles (Fig. 2b and Supplementary Fig. 4a) and since procentriole microtubules are not polyglutamylated[22], the glutamylated tubulin-negative spot of C2cd3 likely represented the procentriole. Staining cells for Sas-6, a marker of procentrioles but not mature centrioles[23], confirmed that C2cd3 is present at procentrioles (Fig. 2c). In mature centrioles, we found C2cd3 slightly distal to the Ninein-or Odf2-marked subdistal appendages (Fig. 2d and Supplementary Fig. 4b). C2cd3 was precisely located between the Cep164-marked distal appendages (Fig. 2e). Finally, the transition zone[25] marker Cep290 was clearly distal to C2cd3 (Fig. 2f), leading us to conclude that C2cd3 is localized near the distal tip of centrioles. CP110 and Ofd1 have also been localized near the distal end of centrioles, with CP110 marking a slightly more distal location than Ofd1 (Ref. 7), namely the centriole cap whose removal allows for elongation of the ciliary axoneme[26]. C2cd3 perfectly co-localized with Ofd1 (Fig. 2g) and was slightly proximal to CP110 (Fig. 2h).

Since C2cd3 co-localizes with Ofd1 and since both of these proteins are mutated in OFD syndromes, we tested whether they physically interact. Using antibodies raised against the endogenous proteins, C2CD3 and OFD1 were found to co-immunoprecipitate out of human RPE cells (Fig. 2i). To further confirm this interaction, GST fusions of Ofd1 fragments were expressed in bacteria, immobilized on beads and used to capture GFP-C2cd3 expressed in HEK cells. Remarkably, the central fragment of Ofd1, which is also responsible for homo-dimerization[27], was found to specifically interact with GFP-C2cd3 (Fig. 2j and Supplementary Fig. 4c). We conclude that C2cd3 forms a complex with Ofd1 at the distal end of centrioles where it co-localizes with other known regulators of centriole elongation such as Centrin[28] or Poc5 (Ref. 29).

Since OFD1 and C2CD3 associate physically and cytologically and their encoding genes are mutated in the same syndrome, we hypothesized that C2cd3 removal would mimic loss of Ofd1 and result in centrin-positive hyperelongation of centrioles[7]. Surprisingly, centrin was undetectable in the vast majority of $C2cd3^{Hty}$ and $C2cd3^{Gt}$ centrioles (Fig. 3a, b) even though total centrin levels stayed constant (Supplementary Fig. 5a), in agreement with a recent study[30]. Similarly, glutamylated tubulin staining failed to reveal centriole hyperelongation in C2cd3 mutant MEFs (Fig. 3c). Thus, unlike loss of Ofd1, loss of C2cd3 does not result in elongation of the distal centriole compartment.

Remarkably, distal appendages (stained by Cep164, Fig. 3c and d) as well as subdistal appendages (stained by Odf2, Fig. 3e and f) were absent from C2cd3 mutant centrioles. Ninein staining confirmed the absence of subdistal appendages and the intactness of the proximal end of centrioles (Supplementary Fig. 5b). Similarly, CPAP, a marker of the proximal segment of centrioles, was retained in *C2cd3* mutants (Fig. 3g and h). Ofd1 levels

were greatly reduced at *C2cd3* mutant centrioles (Fig 3i and j), suggesting that C2cd3 may recruit Ofd1 to centrioles through their physical interaction. While *C2cd3* mutant centrioles lose most markers of the distal centrioles, the centriole cap protein CP110 was still present at the distal end of centrioles (Fig. 3k), concordant with the inability of *C2cd3* cells to assemble a primary cilium[11].

An appealing explanation for the loss of distal centriole structures in *C2cd3* mutant cells is incomplete centriole elongation. Alternatively, it is conceivable that maturation of the distal centriole is affected independently of centriole length alterations. In support of the former hypothesis, the distance between centriole cap and centriole center –measured by fluorescence microscopy– was significantly reduced in $C2cd3^{Gt}$ cells compared to control cells (Fig. 4a,b). To precisely assess the structural defects of *C2cd3* mutant centrioles, we performed thin section electron microscopy on the *C2cd3* MEFs. Confirming our immunofluorescence findings, distal and subdistal appendages were absent from *C2cd3* centrioles (Fig. 4c–e and Supplementary Fig. 6a,b). Total centriole length was precisely assessed by thin-section EM and we found *C2cd3* mutant centrioles to be shorter than controls by ∼150 nm (Fig. 4f). We conclude that C2cd3 is required for the extension of procentrioles into full-length centrioles.

To gain insight into the mechanisms by which C2cd3 controls centriole length, we examined the effects of overexpressing GFP-C2cd3. Strikingly, in RPE cells, we observed one or two juxtanuclear >2 μm-long straight rods marked by GFP-C2cd3 and acetylated microtubules along their length (Fig. 5a, insets) and resistant to nocodazole treatment (Supplementary Fig. 7a). By synchronizing cells in S and releasing in G2[32], we found that 15 to 25% of U2OS cells transfected with GFP-C2cd3 possessed GFP-positive rods, in line with previously described centriole lengthening activities[31,32]. The morphological resemblance to the hyperelongated centrioles from cells overexpressing CPAP or Cep120 (Ref. 3–5,31,32) hinted that the C2cd3 rods might represent hyperelongated centrioles (Fig. 5b–e). These juxtanuclear C2cd3 rods were positive for CPAP and Cep164 at their base (Fig. 5b and c), glutamylated tubulin and centrin along their length (Fig. 5d and e), and showed an enrichment of CP110 at their distal end (Fig. 5e). The absence of the cilium maker IFT88 from the C2cd3 rods (Fig 5d) and the presence of CP110 at the end of these structures (Fig. 5e) strongly suggested that they represent hyperelongated centrioles and not cilia. To confirm that C2cd3 promotes centriole hyperelongation, we imaged the GFP-C2cd3-positive rods by correlative light-electron microscopy[33] (CLEM) and identified continuous extensions of the centriolar microtubules up to 1.3 μm long in three separate cells (Fig. 5f, Supplementary Fig. 7b and Supplementary Video 1).

In addition to hyperelongated centrioles, overexpressed GFP-C2cd3 was found alongside bright microtubules rods (Supplementary Fig. 7c) enriched in acetylated tubulin in various regions of the cytoplasm (Fig. 5a). Similar to prior observations with CPAP overexpression[3], CLEM revealed that these cytoplasmic microtubules structures are reminiscent of centrioles, albeit much less organized. The mixed C2cd3/microtubule rods contained microtubules spaced 250nm apart by an electron dense matrix (Fig. 6a) and doublet microtubules could sometime be distinguished (Fig. 6a, lower panel). Congruently, the C2cd3/microtubule rods were positive for centrin (Fig. 6b). While the biogenesis of

these centriole-like structures is presently unknown, they may have originated and then broken off from hyperelongated centrioles (see Supplementary Fig. 7b and Supplementary Video 1).

The ability of C2cd3 to induce centriole hyperelongation enabled a test of the functional antagonism between C2cd3 and Ofd1. Co-transfection of Ofd1 –but not of a control plasmid– with C2cd3 led to a drastic reduction in the frequency of hyperelongated centrioles (Fig. 5g). Our finding that the OFD gene products Ofd1 and C2cd3 antagonize one another in centriole length regulation suggests a model where C2cd3 promotes centriole lengthening and Ofd1 inhibits the activity of C2cd3 through direct physical contact. In this model, the inhibition exerted by Ofd1 onto C2cd3 would need to be minimal in the early stages of procentriole elongation and increased as centrioles reach their mature length. Further insights may be gained by studying how the centriole lengthening activity of C2cd3 is related to its suggested ability to bind and stabilize microtubules and how C2cd3 function is coordinated with the procentriole elongating activities of CPAP and Cep120 in particular with respect to their microtubule-stabilizing activities[31,32]. Finally, an unexplored aspect of C2cd3 lies in its six canonical C2 domains which are predicted to bind Ca^{2+} and phospholipid headgroups[10]. Centrin, which co-localizes precisely with C2cd3 and promotes centriole lengthening, also binds Ca^{2+} (Ref. 34) and it is tempting to speculate that centriolar Ca^{2+} levels may regulate centriole elongation.

METHODS

Methods and any associated references are available in the online version of the paper.

Online Methods

Research subjects

The consanguineous family and additional families were recruited worldwide based upon the presence of at least one individual with an OFD syndrome proven with oral features (lingual hamartoma, cleft/lobulated tongue, gingival frenulae, and/or cleft lip/palate), facial dysmorphism, and digital anomalies, as well as Meckel syndrome. Whenever possible, individuals underwent a full diagnostic protocol, and a standardized clinical questionnaire was administered to assess the extent of multi-organ involvement. Informed consent was obtained for all participating patients and their families; the study was approved by the Ethics Boards of Necker-Enfants Malades Hospital (Paris) and Dijon University Hospital. In fetuses, pregnancies were terminated after genetic counselling, in accordance with local legislation. Chromosome analysis and clinicopathological examination were performed for all cases. Genomic DNA was extracted from frozen tissue or amniocyte cultured cells in foetal cases, and from peripheral blood samples for patients and their parents using standard procedures.

Genome-wide SNP genotyping and homozygosity mapping

Genome-wide SNP genotyping was performed using the Human Mapping 500K Nsp Array (Affymetrix, Santa Clara, CA) at the Institut de Génétique et de Biologie Moléculaire et Cellulaire (IGBMC, Illkirsch). Sample processing and labeling were performed according to

the manufacturer instructions (Affymetrix GeneChip Mapping 500K Assay Manual, #701930 Rev.3). Hybridization was performed with a GeneChip Hybridization oven 640 at 49°C, 60 rpm for 16 h, washed with a GeneChip Fluidics Station 450, and scanned with a GeneChip Scanner 3000-7G. The image data was processed with the Affymetrix Genotyping Console (GTC v4.1) for determining SNP call and copy-number variation. Homozygosity mapping was performed using HomozygosityMapper[35] default parameters (see **URLs**).

Exome sequencing

Exome capture was performed at the Genoscope Centre National de Génotypage (CNG, Evry) on 8 μg of DNA sample from the affected proband using SureSelect Human All Exon 50Mb kit (Agilent) according to standard procedures. The resulting libraries underwent 2×100-bp paired-end sequencing on an Illumina HiSeq 2000 in accordance with the manufacturer's recommendations.

Reads were aligned to the human reference genome (GRCh37/hg19) with the Burrows-Wheeler Aligner[36] (BWA.0.5.6) and removed potential duplicate paired-end reads using the picardtools.1.22 (see **URLs**). The Genome Analysis Toolkit (GATK) 1.0.57 was used for base quality score recalibration and indel realignment, as well as for single-nucleotide variant and indel discovery and genotyping using standard hard filtering parameters[37,38]. Homozygous variants with quality scores of >30, sequencing depth of >4, quality/depth ratio of >5.0 and strand bias of <-0.10 were conserved from subsequent analyses. Coverage was assessed with the GATK Depth of Coverage tool by ignoring reads with mapping quality of <20 and bases with base quality of <30. Candidate events were then inspected using Integrative Genomics Viewer (IGV). The resulting variants were excluded when the frequency was over 1/1000 in the Exome Variant Server, NHLBI (see **URLs**).

Sanger sequencing validation

Mutation screening of *C2CD3* (NM_015531.4) was performed by direct sequencing of PCR products of the 31 coding exons and the adjacent intronic junctions in 34 patients with OFD. PCR primers (sequences available upon request) were designed with Primer3 (Ref. 39, see **URLs**) according to reference sequence NM_015531.4. PCR products were purified using the Exo-SAP cleanup kit (USB). Sequencing was performed using the ABI BigDye Terminator Cycle Sequencing kit (v3.1) (Applied Biosystems) following the manufacturer's instructions in an ABI 3130 sequencer 7 (Applied Biosystems). Sequence data were analyzed with SeqScape v2.7 (Applied Biosystems). The impact of the missense and splice-site mutation were assessed using PolyPhen-2 (Ref. 40, see **URLs**) and the Human Splicing Finder v.2.4.1 online software[41] (see **URLs**), respectively.

cDNA sequencing

To assess the impact of the c.3911-2A>T substitution on splicing, we extracted total RNA from skin biopsies obtained from patient 2 and two control individuals using the RNeasy Plus Universal Mini Kit (Qiagen), and performed reverse transcription PCR (RT-PCR) using the QuantiTect Reverse Transcription Kit (Qiagen) according to manufacturer's instructions. Analysis of *C2CD3* cDNA was carried out by standard PCR amplification using primers

between exons 20 and 23 as well as between exons 21 and 23, and subsequent Sanger sequencing as described above.

Cell culture

IMCD3 cells were cultured in DMEM/F12 medium (Life Technologies) containing 10% FBS (HyClone) at 37°C in 5% CO2. The medium was supplemented with 0.25% Na_2CO_3 for RPE cells. DMEM with 10% FBS was used to grow HEK293FT and SV40-immortalized MEFs derived from C2cd3 mutant mice and C2cd3 heterozygous mice[11]. To induce ciliogenesis, cells were grown in serum starvation medium (0.2% FBS) for 24 hours. A stable IMCD3 clonal cell line expressing GFP-C2cd3 under control of the EF1α promoter was generated using the Flp-In system (Invitrogen), as described previously[20]. Transfections of RPE, IMCD3 and HEK293 cells were carried out with with X-tremeGENE9 (Roche). U2OS cells were transfected with Lipofectamine 2000. To maximize the centriole elongation frequency observed upon C2cd3 overexpression, 48 h after transfection, U2OS cells were arrested in S phase by addition of hydroxyurea (8 mM) or aphidicolin (2 μg/ml) for 20hr then released into G2 by changing the medium to roscovitine (RO-3306, 10 μM) for 16hr before fixing.

Immunoblotting, immunoprecipitation and immunohistochemistry

All antibodies used in this study are listed in Supplementary table 3. Immunofluorescence was conducted as in Ref. 42. Briefly, cells were fixed for 5 min with 4% PFA and immediately plunged in −20°C methanol before rehydration in PBS and processing for immunofluorescence (except for CPAP immunofluorescence for which the PFA step was omitted). For studying the localization of C2cd3 within centrioles (Fig. 2 and Supplementary Fig. 4), cells were treated with 5 μM nocodazole for 1h before processing for immunofluorescence. All microscopy (except for the measurement of centriole length) was performed with a 63× 1.4 N.A. PlanApo objective mounted on a Zeiss Axio Imager.M1 microscope connected to a Lambda XL light source (Sutter Instruments) and fluorescence was gated by a Sedat filter set (Semrock). Images were captured by a CoolSNAP HQ^2 camera (Photometrics) and the system was controlled by Slidebook 5 (Intelligent Imaging Innovations).

To measure the distance between CP110 and GT335 in MEF cells, z stack images of centrioles were taken on a DeltaVision workstation (GE) equipped with an Olympus PlanApo 60x/1.42 Oil lens and a sCMOS camera and deconvolved using softWoRx software. Only those centrioles with both CP110 and GT335 in the same focal plane were selected for distance measurement. The center points (centroids) of GT335 and CP110 were mapped using SpotTracker plugin in ImageJ and the distances between these two centroids were measured.

Immunoblotting, co-transfection/co-immunoprecipitations and GST capture assays were carried out as before[20,27]. Tandem affinity purification of the BBSome using the RPE-[LAP-BBS4] stable cell line has been described[19].

The immunoprecipitation of endogenous Ofd1 was conducted as follows: two 15 cm dishes of RPE cells were lysed in buffer Co-IP 200 (50 mM Tris pH 7.4, 200 mM NaCl, 1% Triton

X-100, 1mM DTT), the lysate was cleared by centrifugation at 16,000 x *g* and 50 ng of Ofd1 antibody or 2 μg of rabbit IgG were added to 5 mg of cell lysate. After 45min incubation at 4 °C, antibody/antigen complexes were captured on 10 μl of protein A-Sepharose beads through end-over-end incubation for 1h. Beads were washed four times with buffer Co-IP 200 and complexes eluted in NuPage LDS sample buffer (247mM Tris base, 2% LDS, 10% Glycerol, 0.51 mM EDTA, 0.22 mM Coomassie G250, 0.175 mM Phenol Red, pH 8.5).

Electron microscopy

Cells were seeded on 8-well Permanox chamber slides (Nalgene Nunc International, Naperville, IL) and were subsequently fixed in 3.5 % glutaraldehyde in 0.1 M phosphate buffer (PB) for 10 minutes at 37 °C, replaced with fresh pre-warmed 3.5% glutaraldehyde and incubated 1 hour at 4 °C. Cells were postfixed in 2% OsO_4 for 1 hour at room temperature and stained in 2% uranyl acetate in the dark for 2 h at 4 °C. Finally, cells were rinsed in distilled water, dehydrated in ethanol, and embedded overnight in Durcupan resin (Fluka, Sigma-Aldrich, St. Louis, USA). Following polymerization, serial ultrathin sections (0.06 – 0.08 μm) were cut with an UC-6 Ultracut (Leica, Heidelberg, Germany) and stained with lead citrate. Photomicrographs were obtained under a FEI Tecnai G2 Spirit transmission electron microscope (FEI Europe, Eindhoven, Netherlands) using a Morada digital camera (Olympus Soft Image Solutions GmbH, Münster, Germany). Quantitative measurements of centriole length were determined in longitudinal sections using Fiji.

Correlative Light-Electron Microscopy (CLEM)

U2OS cells were seeded onto photo-etched gridded coverslips (Bellco) and transfected with pEGFP-C2cd3 either alone or in combination with pRFP-PACT. 48h after transfection, cells were fixed with glutaraldehyde as above and the regions of interest (ROIs) were identified on an inverted fluorescence microscope (Deltavision, GE Healthcare). The coordinates of each ROI were recorded at low magnification to enable identification of the ROI after embedding. Processing of samples for EM was performed as above except for the insertion of a block trimming step as described in [33]. Serial sections were aligned using the TrakEM2 plugin [43] from Fiji [44].

URLs

HomozygosityMapper, http://www.homozygositymapper.org/

Human Splicing Finder, http://www.umd.be/HSF/

PolyPhen-2, http://genetics.bwh.harvard.edu/pph2/

NHLBI Exome Sequencing Project (ESP) Exome Variant Server, http://evs.gs.washington.edu/EVS/

Primer3, http://bioinfo.ut.ee/primer3-0.4.0/primer3/

Picard, http://picard.sourceforge.net/

Protein Homology/analogY Recognition Engine V 2.0, http://www.sbg.bio.ic.ac.uk/phyre2/html/page.cgi?id=index

REFERENCE SEQUENCES

C2CD3 cDNA sequence (NM_015531.4) C2CD3 protein sequence (NP_056346.3)

Supplementary Material

Refer to Web version on PubMed Central for supplementary material.

ACKNOWLEDGMENTS

We thank Laurence Pelletier, Michel Bornens, Carsten Janke, Tim Stearns and Sophie Saunier for antibodies, Aimin Liu for the C2cd3 mutant MEFs and the C2cd3 cDNA, Jeremy Reiter for the Ofd1 cDNA, Sean Munro for pRFP-PACT, Vincent Meyer (Genoscope, CNG), Tara Hardy (U. Leicester) and Nadia Elkhartoufi (Necker, Paris) for technical support, Forrest Collman (Stanford) for help with the serial alignment, members from the Nachury lab for helpful discussions and the patients and their families for their participation. This work was supported by grants from NIGMS (GM089933 to M.V.N.), the GIS-Institut des Maladies Rares (HTS), the French Ministry of Health (PHRC national 2010-A01014-35), the Regional Council of Burgundy (to C.T-R), The Wellcome Trust and Kidney Research UK (to A.M.F) and the Fondazione Telethon (TGM11CB3) and the European Community's Seventh Framework Programme [FP7/2007-2013; #241955] (to B.F.). We also thank the NHLBI GO Exome Sequencing Project (see **URLs**) and its ongoing studies which produced and provided exome variant calls for comparison: the Lung GO Sequencing Project (HL-102923), the WHI Sequencing Project (HL-102924), the Broad GO Sequencing Project (HL-102925), the Seattle GO Sequencing Project (HL-102926) and the Heart GO Sequencing Project (HL-103010).

REFERENCES

1. Bornens M, Paintrand M, Moudjou M, Delacroix H. Centrosome organization and centriole architecture: their sensitivity to divalent cations. J Struct Biol. 1992; 108:107–128. [PubMed: 1486002]
2. Bettencourt-Dias M, Glover DM. Centrosome biogenesis and function: centrosomics brings new understanding. Nat Rev Mol Cell Biol. 2007; 8:451–463. [PubMed: 17505520]
3. Kohlmaier G, et al. Overly long centrioles and defective cell division upon excess of the SAS-4-related protein CPAP. Curr Biol. 2009; 19:1012–1018. [PubMed: 19481460]
4. Tang C-JC, Fu R-H, Wu K-S, Hsu W-B, Tang TK. CPAP is a cell-cycle regulated protein that controls centriole length. Nat Cell Biol. 2009; 11:825–831. [PubMed: 19503075]
5. Schmidt TI, et al. Control of centriole length by CPAP and CP110. Curr Biol. 2009; 19:1005–1011. [PubMed: 19481458]
6. Ferrante MI, et al. Identification of the gene for oral-facial-digital type I syndrome. Am J Hum Genet. 2001; 68:569–576. [PubMed: 11179005]
7. Singla V, Romaguera-Ros M, García-Verdugo JM. Ofd1, a Human Disease Gene, Regulates the Length and Distal Structure of Centrioles. Dev Cell. 2010; 18:410–424. [PubMed: 20230748]
8. Gurrieri F, Franco B, Toriello H, Neri G. Oral-facial-digital syndromes: review and diagnostic guidelines. Am J Med Genet A. 2007; 143A:3314–3323. [PubMed: 17963220]
9. Patel S, Barkovich AJ. Analysis and classification of cerebellar malformations. AJNR Am J Neuroradiol. 2002; 23:1074–1087. [PubMed: 12169461]
10. Zhang D, Aravind L. Novel transglutaminase-like peptidase and C2 domains elucidate the structure, biogenesis and evolution of the ciliary compartment. Cell Cycle. 2012; 11:3861–3875. [PubMed: 22983010]
11. Hoover AN, et al. C2cd3 is required for cilia formation and Hedgehog signaling in mouse. Development. 2008; 135:4049–4058. [PubMed: 19004860]

12. Zohn IE, Anderson KV, Niswander L. Using genomewide mutagenesis screens to identify the genes required for neural tube closure in the mouse. Birth Defects Res. Part A Clin. Mol. Teratol. 2005; 73:583–590.
13. Poretti A, et al. Delineation and diagnostic criteria of Oral-Facial-Digital Syndrome type VI. Orphanet journal of rare diseases. 2012; 7:4. [PubMed: 22236771]
14. Srour M, et al. Mutations in C5ORF42 cause Joubert syndrome in the French Canadian population. Am J Hum Genet. 2012; 90:693–700. [PubMed: 22425360]
15. Lopez E, et al. C5orf42 is the major gene responsible for OFD syndrome type VI. Hum Genet. 2013
16. Thomas S, et al. TCTN3 Mutations Cause Mohr-Majewski Syndrome. The American Journal of Human Genetics. 2012; 91:372–378. [PubMed: 22883145]
17. Dammermann A, Merdes A. Assembly of centrosomal proteins and microtubule organization depends on PCM-1. J Cell Biol. 2002; 159:255–266. [PubMed: 12403812]
18. Kim JC, et al. The Bardet-Biedl protein BBS4 targets cargo to the pericentriolar region and is required for microtubule anchoring and cell cycle progression. Nat Genet. 2004; 36:462–470. [PubMed: 15107855]
19. Nachury MV, et al. A core complex of BBS proteins cooperates with the GTPase Rab8 to promote ciliary membrane biogenesis. Cell. 2007; 129:1201–1213. [PubMed: 17574030]
20. Jin H, et al. The conserved Bardet-Biedl syndrome proteins assemble a coat that traffics membrane proteins to cilia. Cell. 2010; 141:1208–1219. [PubMed: 20603001]
21. Lopes CAM, et al. Centriolar satellites are assembly points for proteins implicated in human ciliopathies, including oral-facial-digital syndrome 1. J Cell Sci. 2011; 124:600–612. [PubMed: 21266464]
22. Kleylein-Sohn J, et al. Plk4-induced centriole biogenesis in human cells. Dev Cell. 2007; 13:190–202. [PubMed: 17681131]
23. Strnad P, et al. Regulated HsSAS-6 levels ensure formation of a single procentriole per centriole during the centrosome duplication cycle. Dev Cell. 2007; 13:203–213. [PubMed: 17681132]
24. Mogensen MM, Bornens M, Malik A, Piel M, Bouckson-Castaing V. Microtubule minus-end anchorage at centrosomal and non-centrosomal sites: the role of ninein. J Cell Sci. 2000; 113(Pt 17):3013–3023. [PubMed: 10934040]
25. Garcia-Gonzalo FR, Reiter JF. Scoring a backstage pass: mechanisms of ciliogenesis and ciliary access. J Cell Biol. 2012; 197:697–709. [PubMed: 22689651]
26. Spektor A, Tsang WY, Khoo D, Dynlacht BD. Cep97 and CP110 suppress a cilia assembly program. Cell. 2007; 130:678–690. [PubMed: 17719545]
27. Giorgio G, et al. Functional characterization of the OFD1 protein reveals a nuclear localization and physical interaction with subunits of a chromatin remodeling complex. Mol Biol Cell. 2007; 18:4397–4404. [PubMed: 17761535]
28. Salisbury JL, Suino KM, Busby R, Springett M. Centrin-2 is required for centriole duplication in mammalian cells. Curr Biol. 2002; 12:1287–1292. [PubMed: 12176356]
29. Azimzadeh J, et al. hPOC5 is a centrin-binding protein required for assembly of full-length centrioles. J Cell Biol. 2009; 185:101–114. [PubMed: 19349582]
30. Balestra FR, Strnad P, Flückiger I, Gönczy P. Discovering Regulators of Centriole Biogenesis through siRNA-Based Functional Genomics in Human Cells. Dev Cell. 2013; 25:555–571. [PubMed: 23769972]
31. Lin Y-N, et al. CEP120 interacts with CPAP and positively regulates centriole elongation. J Cell Biol. 2013; 202:211–219. [PubMed: 23857771]
32. Comartin D, et al. CEP120 and SPICE1 Cooperate with CPAP in Centriole Elongation. Curr Biol. 2013; 23:1360–1366. [PubMed: 23810536]
33. Reddick LE, Alto NM. Correlative Light and Electron Microscopy (CLEM) as a Tool to Visualize Microinjected Molecules and their Eukaryotic Sub-cellular Targets. JoVE (Journal of Visualized Experiments). 2012:e3650–e3650. [PubMed: 22588091]

34. Thompson JR, Ryan ZC, Salisbury JL, Kumar R. The structure of the human centrin 2-xeroderma pigmentosum group C protein complex. J Biol Chem. 2006; 281:18746–18752. [PubMed: 16627479]

References for Online Methods

35. Seelow D, Schuelke M, Hildebrandt F, Nurnberg P. HomozygosityMapper--an interactive approach to homozygosity mapping. Nucleic Acids Res. 2009; 37:W593–W599. [PubMed: 19465395]

36. Li H, Durbin R. Fast and accurate short read alignment with Burrows-Wheeler transform. Bioinformatics. 2009; 25:1754–1760. [PubMed: 19451168]

37. McKenna A, et al. The Genome Analysis Toolkit: a MapReduce framework for analyzing next-generation DNA sequencing data. Genome Res. 2010; 20:1297–1303. [PubMed: 20644199]

38. DePristo MA, et al. A framework for variation discovery and genotyping using next-generation DNA sequencing data. Nat Genet. 2011; 43:491–498. [PubMed: 21478889]

39. Koressaar T, Remm M. Enhancements and modifications of primer design program Primer3. Bioinformatics. 2007; 23:1289–1291. [PubMed: 17379693]

40. Adzhubei IA, et al. A method and server for predicting damaging missense mutations. Nat Methods. 2010; 7:248–249. [PubMed: 20354512]

41. Desmet F-O, et al. Human Splicing Finder: an online bioinformatics tool to predict splicing signals. Nucleic Acids Res. 2009; 37:e67. [PubMed: 19339519]

42. Breslow DK, Koslover EF, Seydel F, Spakowitz AJ, Nachury MV. An in vitro assay for entry into cilia reveals unique properties of the soluble diffusion barrier. J Cell Biol. 2013; 203:129–147. [PubMed: 24100294]

43. Cardona A, et al. TrakEM2 software for neural circuit reconstruction. PLoS ONE. 2012; 7:e38011. [PubMed: 22723842]

44. Schindelin J, et al. Fiji: an open-source platform for biological-image analysis. Nat Methods. 2012; 9:676–682. [PubMed: 22743772]

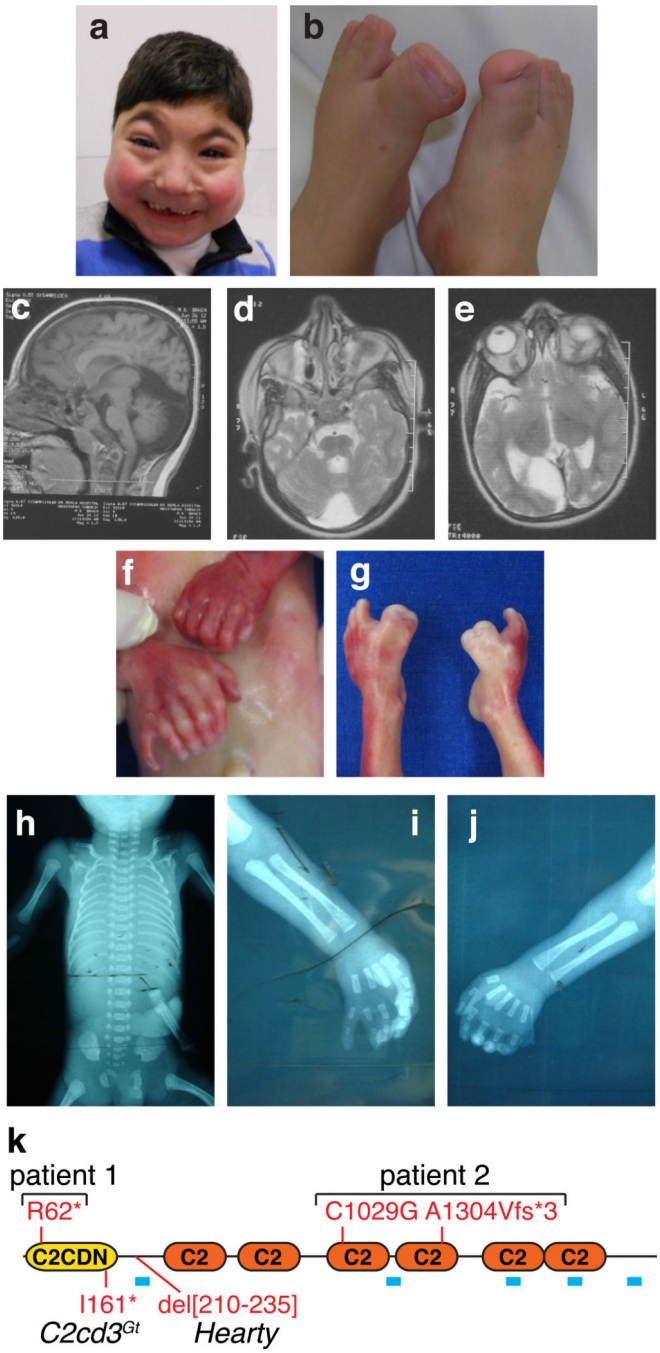

Figure 1. Clinical presentations of OFD patients with mutations in *C2CD3*

(a–e) Characterization of the 4 year-old patient (case 1) showing microcephaly with trigonocephaly, facial dysmorphism including telecanthus, up-slanting palpebral fissures and microretrognathia (a), bilateral broad duplicated and deviated hallux (b), and brain MRI with corpus callosum hypoplasia (c), MTS (d), subarachnoid cysts in the right occipital lobe and the posterior fossa (d,e), and incomplete myelinisation of the white matter (c–e). Informed consent was obtained from the patient's family.

(f–j) Pictures of the 22 wg fetus (case 2) showing bilateral hand postaxial polydactyly (f) and broad duplicated hallux (g), and X-rays with normal thorax (h) and postaxial polydactyly of the hands (i,j).

(k) Domain organization of C2CD3 (C2 calcium-dependent domain containing 3). The six orange ovals correspond to canonical PKC-C2 domains and the yellow oval is the signature C2CD3N–C2 domain[10] . Patient mutations are indicated in red on top of the diagram, mouse mutants are displayed under the diagram and peptides identified in LAP-BBS4 preparations are mapped onto the diagram by blue bars. The splice site mutation c.3911-2A>T leads to a four nucleotide frameshift deletion (c.3911_3914delCAAG) predicted to result in a premature stop codon at position 1307.

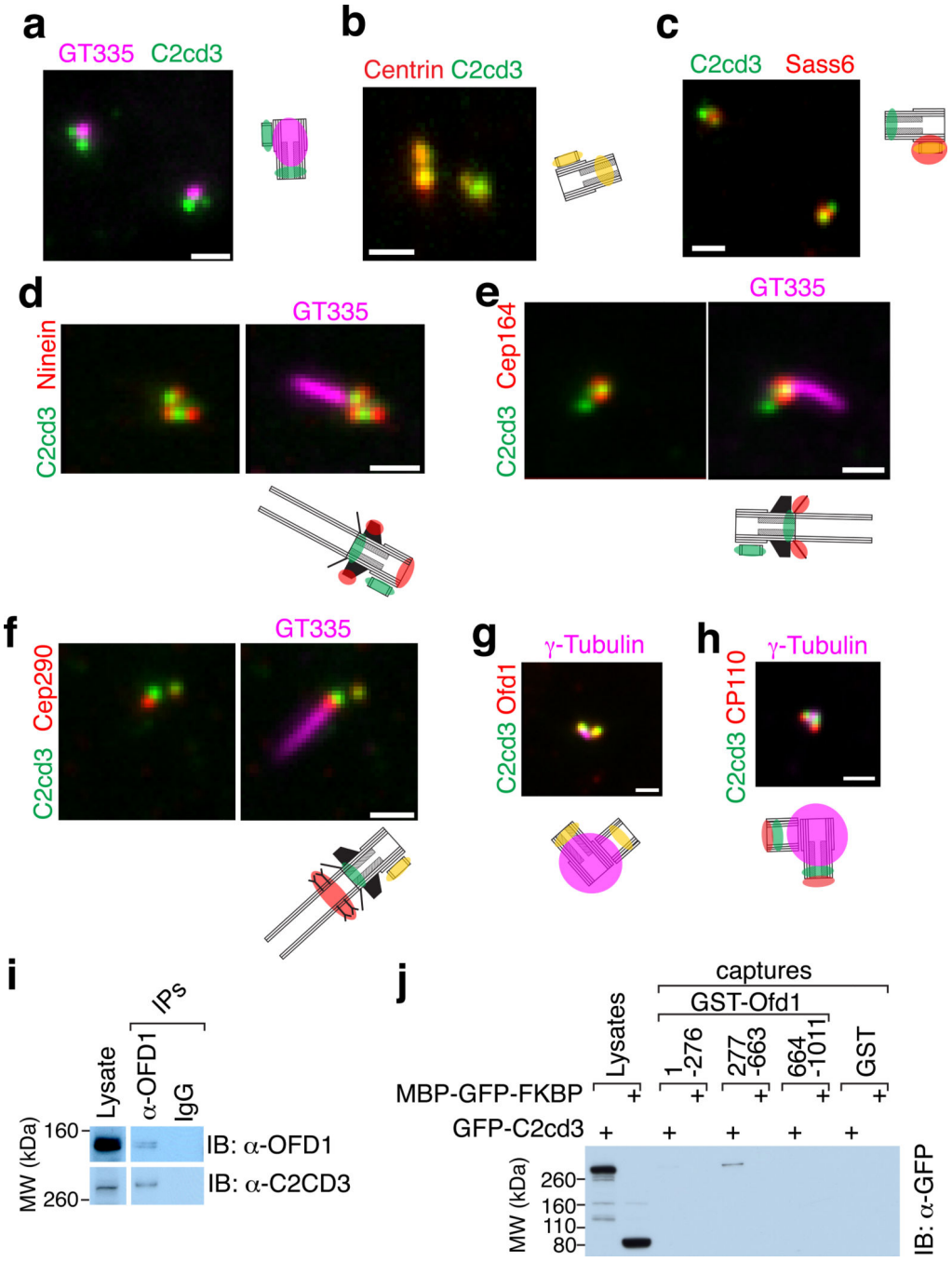

Figure 2. C2cd3 co-localizes with Ofd1 at the distal end of centrioles and procentrioles and physically interacts with Ofd1

IMCD3-[GFP-C2cd3] cells stained for:

(a) The centriolar marker branched-glutamylated tubulin (GT335, pink).

(b) The distal centriole and procentriole marker Centrin (red).

(c) The procentriole marker Sass6 (red).

(d) Ninein (red, marks the subdistal appendages and the proximal end of the centrioles and procentrioles) and glutamylated tubulin (GT335, pink, marks the ciliary axoneme).

(e) Cep164 (red, marks the distal appendages) and glutamylated tubulin (GT335, pink).

(f) Cep290 (red, marks the transition zone) and glutamylated tubulin (GT335, pink).
(g) Ofd1 (red) and γ-tubulin (pink, marks the pericentriolar material near the proximal part of the centriole).
(h) The distal cap marker CP110 (red) and γ-tubulin (pink).
All cells were treated with nocodazole before processing for immunofluorescence. All scale bars are 1 μm.
(i) Immunoprecipitation of OFD1 from RPE cell extract recovers C2CD3. For the C2CD3 immunoblot, 160 equivalent of eluates and 1 equivalent of lysate were ran on the gel. For the OFD1 immunoblot, 4 equivalent of eluates and 1 equivalent of lysate were ran on the gel. The eluate and lysate panels are cropped from the same film exposure.
(j) GST capture assays. GFP-C2cd3 and MBP-GFP-FKBP (negative control) expressed in HEK cells were captured by bacterially expressed GST fusions to Ofd1 fragments. Captured proteins were detected by immunoblotting for GFP. 80 equivalent of eluates and 1 equivalent of lysate were ran on the gel.

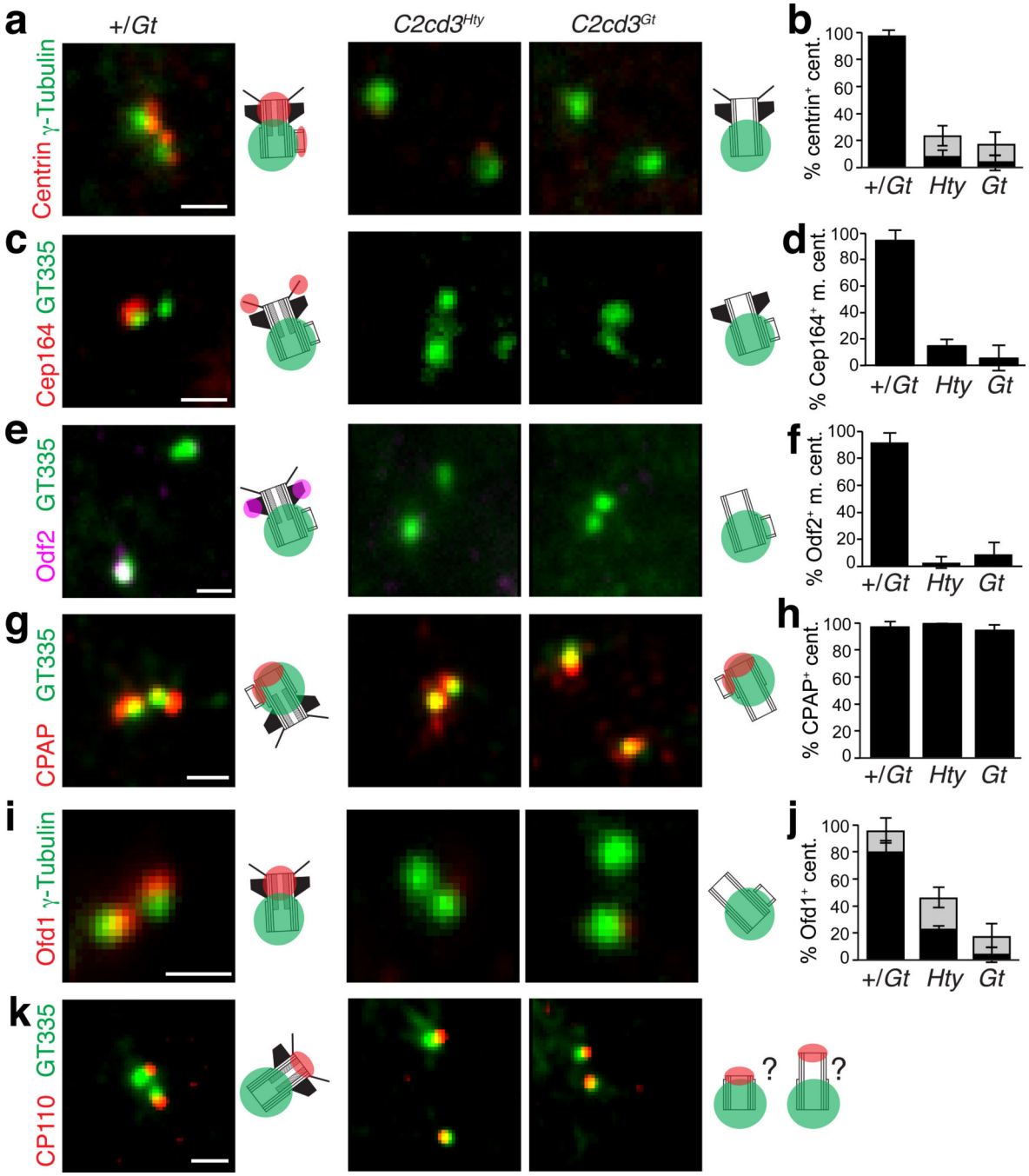

Figure 3. Loss of C2cd3 results in the disappearance of distal centriole structures

(a) MEFs derived from heterozygous (+/*Gt*) and homozygous C2cd3 mutant mice (C2cd3^{Hty} and C2cd3^{Gt}) were stained for γ-tubulin (green) and centrin (red).

(b) Counting of centrin-positive centrioles. Black bars correspond to centrioles strongly positive for centrin (as in the left panel of a), grey bars are for centrioles weakly positive for centrin (as the centriole in the lower right corner of the middle panel of a). Error bars denote standard deviations between microscopy fields. Centrioles were identified by γ-tubulin staining. At least 50 cells of each genotype were counted.

(c) MEFs were stained for polyglutamylated tubulin (GT335, green) and Cep164 (red).
(d) Counting of Cep164-positive mother centrioles. Error bars denote standard deviations between microscopy fields. Cells with at least one spot of Cep164 colocalizing with GT335 were counted as Cep164-positive mother centrioles. At least 50 cells of each genotype were counted.
(e) MEFs were stained for polyglutamylated tubulin (GT335, green) and Odf2 (pink).
(f) Counting of Odf2-positive mother centrioles. Error bars denote standard deviations between microscopy fields. Cells with at least one spot of Odf2 colocalizing with GT335 were counted as Odf2-positive mother centrioles. At least 50 cells of each genotype were counted.
(g) MEFs were stained for γ-tubulin (green) and CPAP (red). CPAP location to the proximal end of centrioles and procentrioles leads to an overlap in signals at these two locations and only one diffraction limited spot of CPAP detected.
(h) Counting of CPAP-positive centrioles. Error bars denote standard deviations between microscopy fields. Centrioles were identified by GT335 staining. At least 50 cells of each genotype were counted.
(i) MEFs were stained for γ-tubulin (green) and Ofd1 (red).
(j) Counting of Ofd1-positive centrioles. Black bars correspond to centrioles strongly positive for Ofd1, grey bars are for centrioles weakly positive for Ofd1. Error bars denote standard deviations between microscopy fields. Centrioles were identified by GT335 staining. At least 50 cells of each genotype were counted.
(k) MEFs were stained for polyglutamylated tubulin (GT335, green) and CP110 (red).
All scale bars are 1 μm.

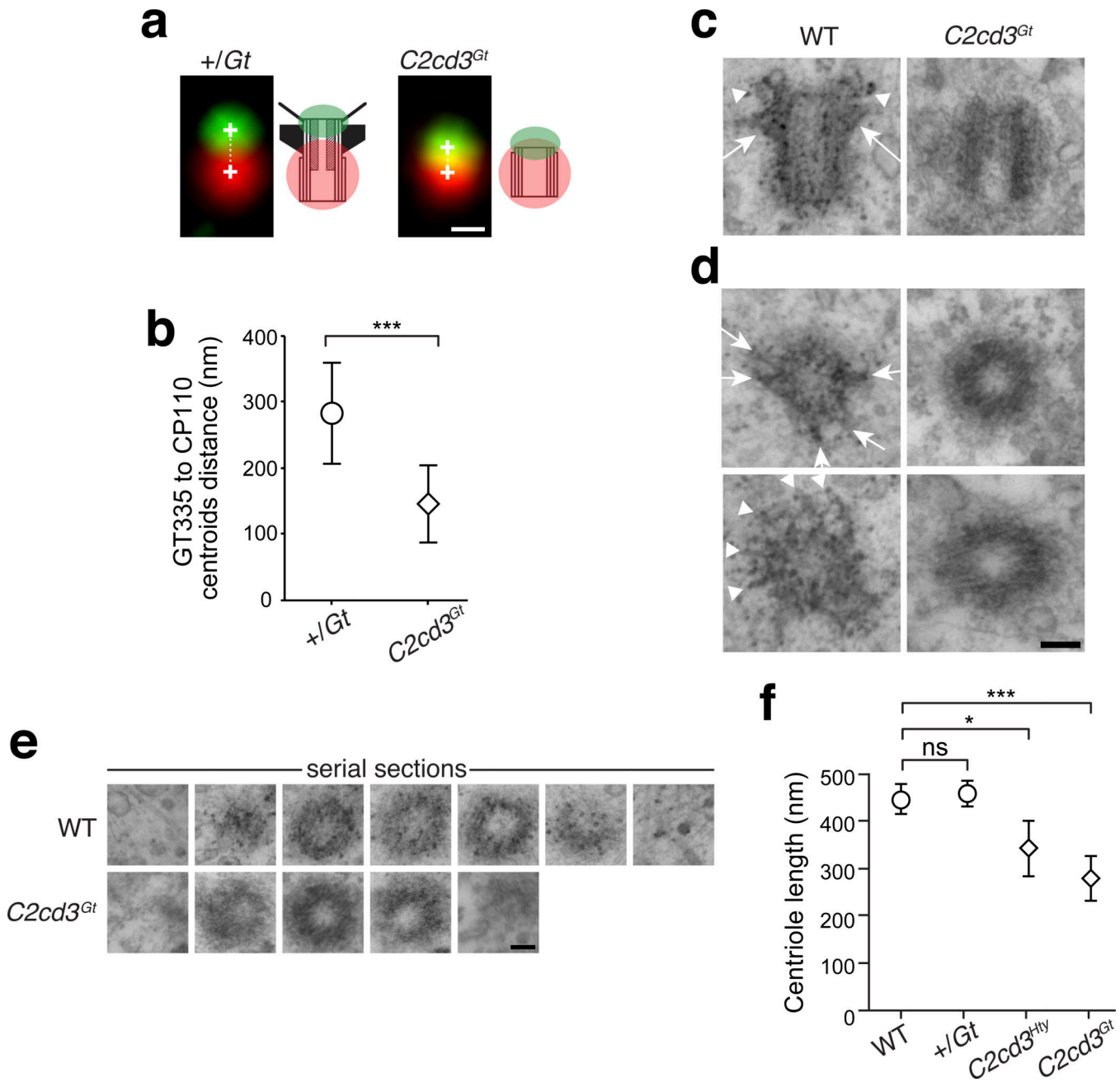

Figure 4. *C2cd3* is required for centriole elongation

(a) Gallery of centrioles stained for CP110 (red) and GT335 (green) with the centroid of each fluorescent spot shown as a white cross. Images were deconvolved. Scale bar 0.2 μm. (b) An estimate of centriole length was obtained from the distance between the centroid of the GT335 spot and the centroid of the CP110 spot. 17 control cells and 27 *C2cd3*^{Gt} cells were measured. The asterisks denote a highly significant difference ($p<10^{-4}$) by Student t-test.

(c) Longitudinal and (d) transverse TEM sections of WT and *C2cd3*^{Gt} centrioles. Centrioles from the mutant MEFs appear stunted and lack all appendages (arrows point to subdistal appendages and arrowheads point to distal appendages). Scale bar 100 nm.
(e) Serial transverse TEM sections of WT and *C2cd3*^{Gt} centrioles. WT centrioles are contained within 5 to 6 sections whereas *C2cd3*^{Gt} centrioles span less than 3 sections. Scale bar 100 nm.
(f) Measurement of centriole length using data collected from 4 WT, 14 +/Gt, 6 *C2cd3*^{Hty} and 10 *C2cd3*^{Gt} centrioles. The error bar denotes one standard deviation. Three asterisks denote a highly significant difference ($p<10^{-4}$) by Student t-test and one asterisk a significant difference ($p<10^{-1}$) by Student t-test.

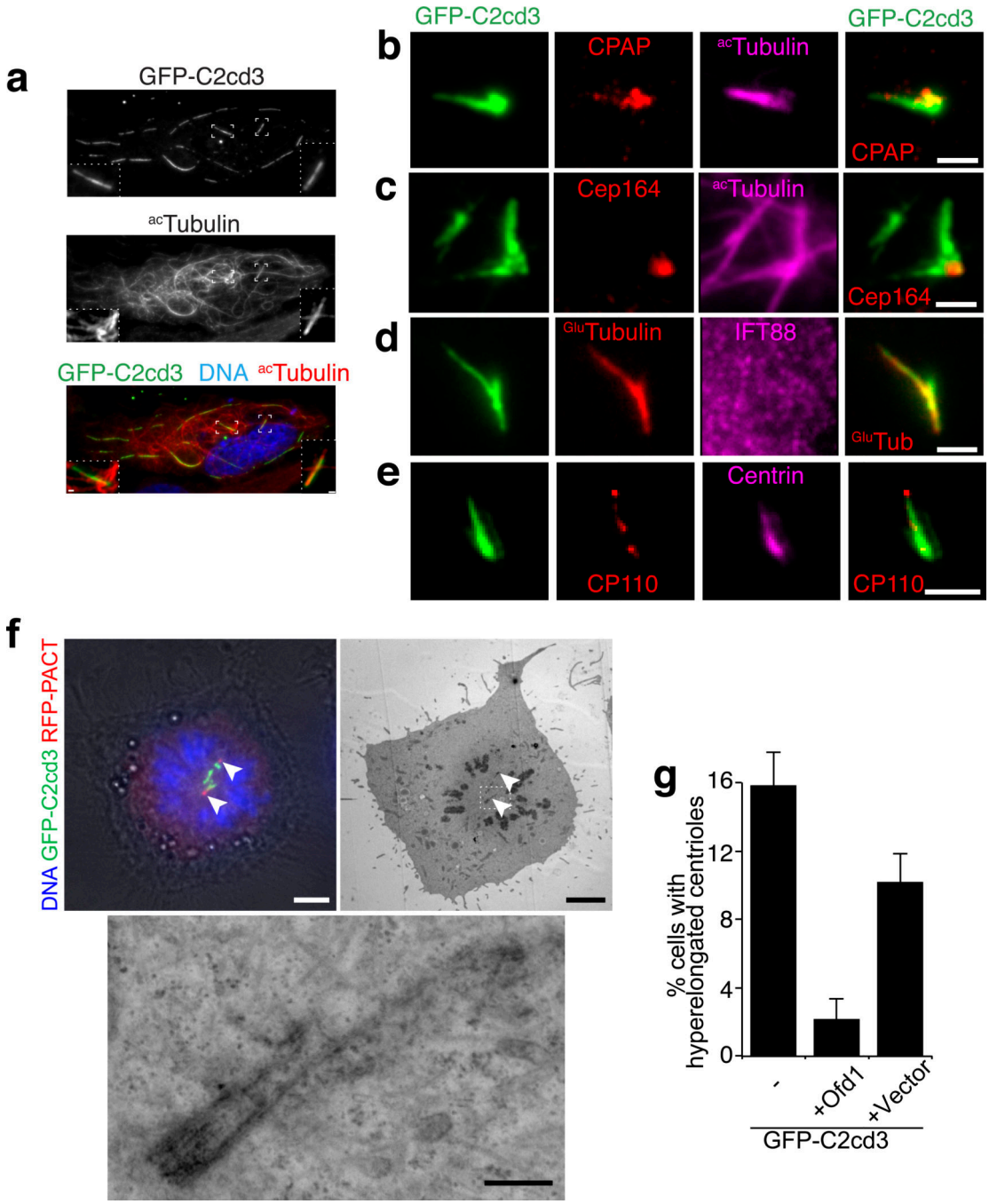

Figure 5. Ofd1 antagonizes the centriole-elongating activity of C2cd3

(a) RPE cells transfected with GFP-C2cd3 were stained or acetylated tubulin (red) and DNA (blue). GFP-C2cd3 colocalizes extensively with acetylated microtubules, in particular at two straight juxtanuclear rods (insets). Scale bar 5 μm.

(b–e) U2OS osteosarcoma cells transfected with GFP-C2cd3 and subjected to a block in S phase and release into G2 were stained for CPAP (red, c) and acetylated tubulin (magenta, c), Cep164 (red, d) and acetylated tubulin (magenta, d), glutamylated tubulin (GT335, red,

e) and IFT88 (magenta, e) and CP110 (red, f) and centrin (magenta, f). The contrast in the IFT88 channel was maximized to reveal background levels of staining. Scale bars 2 μm.
(f) Correlative light electron microscopy of an elongated GFP-C2cd3 filament connected to the centriole. The centrosomes (arrowhead) were located using a fusion of the Red Fluorescent Protein (RFP) with the Pericentrin/AKAP450 Centrosome Targeting domain (PACT). The cell of interest was first imaged by fluorescence (left panel) and located in thin sections imaged by electron microscopy (right panel). Serial sections were aligned and projected to show centriole hyperelongation (lower panel). Individual sections are shown in Supplementary Figure 7b and Supplementary Video 1. Scale bar 5 μm (upper panels), 200 nm (lower panel).
(g) U2OS osteosarcoma cells were transfected with GFP-C2cd3 alone, GFP-C2cd3 and Myc-Ofd1 or GFP-C2cd3 and an empty Myc plasmid. Cells were stained for Cep164 and Myc and hyperelongated centrioles were scored in cells positive for GFP and Myc. At least 70 cells were counted for each condition. The error bars represent the standard deviations between four independent experiments.

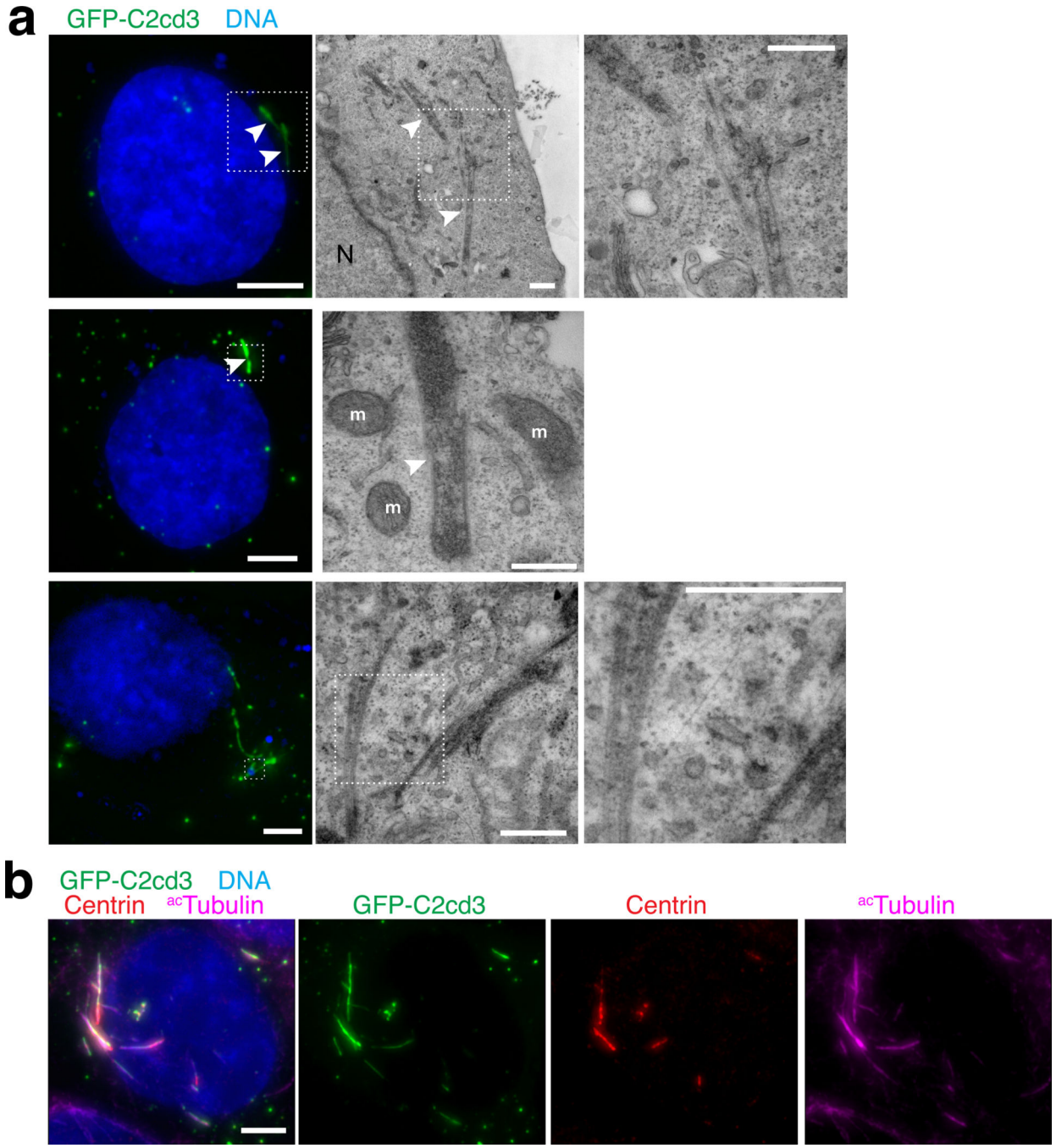

Figure 6. C2cd3 promotes assembly of microtubule structures with centriolar features

(a) CLEM of cytoplasmic GFP-C2cd3 filaments. N, nucleus; m, mitochondria. Scale bar 5 μm (fluorescence panels), 500 nm (EM panels).

(b) U2OS osteosarcoma cells transfected with GFP-C2cd3 were stained for centrin (red), acetylated tubulin (magenta) and DNA (blue). Scale bar 5 μm.